Photoluminescence and electrical properties in Pr-modified (Ba$_{1-x}$Ca$_x$)TiO$_3$ multifunctional ceramics

Miroslaw M. Bućko[1], Agnieszka Wilk[1], Jerzy Lis[1], Anna Toczek[1], Lucjan Kozielski[2,*]

[1]*AGH – University of Science and Technology, Faculty of Materials Science and Ceramics, al. Mickiewicza 30, 30-059 Krakow, Poland*
[2]*Faculty of Science and Technology, Institute of Materials Engineering, University of Silesia, 1A 75 Pułku Piechoty St., 41-500 Chorzów, Poland*

Abstract

Mechanoluminescence materials, characterized with non-thermal light emission in response to mechanical stimuli, can have many applications in direct conversion of mechanical energy into light energy. The aim of this study was to develop wet chemistry approaches for the synthesis of the finest ceramic powders of barium calcium titanate for the use in the production of a mechanoluminescent detector. Wet chemistry route allows the control of the particle size of ceramic materials up to several nanometers. For the first time luminescence was recorded in Ba$_{0.9}$Ca$_{0.1}$TiO$_3$ ceramics despite reports that light emission in BCT is possibly only over 23% of calcium content. The resulting ceramics showed high relative density, reasonable ferro and dielectric properties, and red light emission can be observed with the naked eye.

Keywords: lead-free BCT ceramics, wet chemistry method, mechanoluminescence, dielectric properties

I. Introduction

Mechanoluminescence (ML) is a non-thermal emission of light in response to mechanical stimuli, so that ML materials can have a lot of applications in the direct conversion of mechanical into light energy. When the ML layer covers the monitored structure, the image of the entire surface emission recorded by the cameras reflects dynamic forces and stress distribution, so it can act as a remote visual mechanical sensor of the dynamical forces and stress distribution. Due to this optical technique for mechanically weak points detection, the ML surface layer can early reveal danger of destruction and later final crack propagation. Consequently, ML materials have been used for structural health monitoring (SHM) of buildings [1–3], bridges [4,5] as well as welding points of metal constructions and pipelines [6]. Additionally, a novel information storage and visual expression devices based on ML are also very attractive for consumer electronics market [7].

These materials are also extremely interesting from a scientific point of view, because of the piezoelectric and optical properties occurring simultaneously in one intelligent structure. However, the ML phenomenon itself remains still unclear [8].

Barium titanate with the chemical formula BaTiO$_3$ (BT) is a well-known lead-free piezoelectric material with the perovskite structure discovered very early. BT has a relatively high piezoelectric constant so it can even be used for actuator applications [9,10]. The BT perovskite structure is very tolerant to variations in the composition and even defects due to its adaptation ability to the lack of A–O and B–O bond. Consequently, the centre of positive and negative charges in the unit cell is no longer in equilibrium, resulting in creation of the polarization vector and piezoelectric effect [11]. These variations frequently involve changes in the crystal symmetry when one or more cations shift from high-symmetry space in the lattice [12,13]. Preparation of a solid solution of barium titanate - calcium titanate (BCT) leads to further improvement of piezoelectric properties [14,15], comparable with potassium sodium niobate KNN [16].
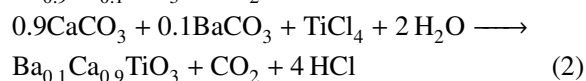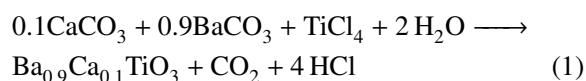
However, even though barium titanate is one of the very early discovered perovskites, new processing and

---

*Corresponding author: tel: +48 32 2691870,
e-mail: *lucjan.kozielski@us.edu.pl*

sintering methods are still part of active research to improve the final properties, because of environmental restriction for the lead contained PZT. In this study BCT powders were produced by new chemical route. Finally, the improved dielectric properties and piezoelectric coefficients were achieved. Additionally, for the first time luminescence was recorded in $Ba_{0.9}Ca_{0.1}TiO_3$ despite reports that light emission in BCT is possible only in barium calcium titanate with over 23% of calcium content [17].

II. Experimental details

In this work a new wet chemistry method was used for the preparation of Pr-doped BCT ceramic powders, i.e. $Ba_{0.898}Ca_{0.1}Pr_{0.002}TiO_3$ (B9C1TO) and $Ba_{0.098}Ca_{0.9}Pr_{0.002}TiO_3$ (B1C9TO) samples. The authors successfully applied co-precipitation and calcination of precursors ($BaCO_3$ and $CaCO_3$ from POCH-Avantor Performance Materials) using ammonium oxalates and the thermal decomposition of the obtained organometallic precursors of ethylene diaminetetra acetic acid (EDTA) and citric acid. Appropriate quantities of $BaCO_3$ and $CaCO_3$ powders were measured on the analytical balance to the nearest 0.001 g in the amount calculated according to the reactions:

$$0.1CaCO_3 + 0.9BaCO_3 + TiCl_4 + 2\,H_2O \longrightarrow$$
$$Ba_{0.9}Ca_{0.1}TiO_3 + CO_2 + 4\,HCl \qquad (1)$$
$$0.9CaCO_3 + 0.1BaCO_3 + TiCl_4 + 2\,H_2O \longrightarrow$$
$$Ba_{0.1}Ca_{0.9}TiO_3 + CO_2 + 4\,HCl \qquad (2)$$

The weighed substrates were completely dissolved in concentrated hydrochloric acid and a sufficient amount of 0.998 M $TiCl_4$ (Sigma-Aldrich) was added. Praseodymium oxide (Pr_6O_{11}) (Sigma-Aldrich) was then dissolved in hot nitric acid in the amount of $y = 0.002$, calculated using the formula $Ba_{x-y}Ca_{1-x}Pr_yTiO_3$ (where $x = 0.1$ and 0.9). The prepared adenosine admixture was added to the solution of Ba^{2+}, Ca^{2+} and Ti^{4+} cations. Each solution was diluted with distilled water

to the same volume of 500 cm³. Using a method of co-precipitation with saturated ammonium oxalate, 20 g of both compounds were prepared. The samples were calcined separately at 1000 °C with a constant temperature rise of 5 °C/min and hold period at maximum temperature of 2 h.

The calcined powders were then homogenized by milling in an attrition mill for 1 h using milling media made of ZrO_2 in anhydrous propanol. After adding 1% of plasticizer to the mortar, disks with a diameter of 10 mm were prepared by uniaxial compression. The pressed samples were heat treated at 400 °C and held for 30 min to burn off organic matter. They were then heated with a constant temperature rise of 5 °C/min to 1500 °C and kept at a maximum temperature for 2 h. The samples were placed in a platinum crucible in the air during sintering.

To determine the shrinkage of the samples during the sintering, the diameters of green and sintered discs were measured with an optical microscope (Leica M32) and the microstructure was examined with NOVA NANO 200 SEM. Microstructural analysis was done using a scanning electron microscope (SEM) and the grain size on the observed surface (after chemical etching) was measured by the linear intercept method using a conversion factor of 1 776.24 and the average size was calculated from measurements of 300 grains. The phase composition of the obtained BCT samples was analysed by X-ray diffraction (PANalytical X'PertPro multifunctional diffractometer). The Rietveld refining method was used to determine the size of unit cells.

Dielectric and ferroelectric properties were measured using Quadtech 7600 Plus Precision LCR Meter. Luminescence spectra were recorded at room temperature on a Spex Fluorolog 2 spectrofluorometer.

III. Results and discussion

3.1. Microstructural investigation

Figure 1 shows SEM images of the etched surfaces of the prepared BCT ceramics. The B1C9TO ceram-
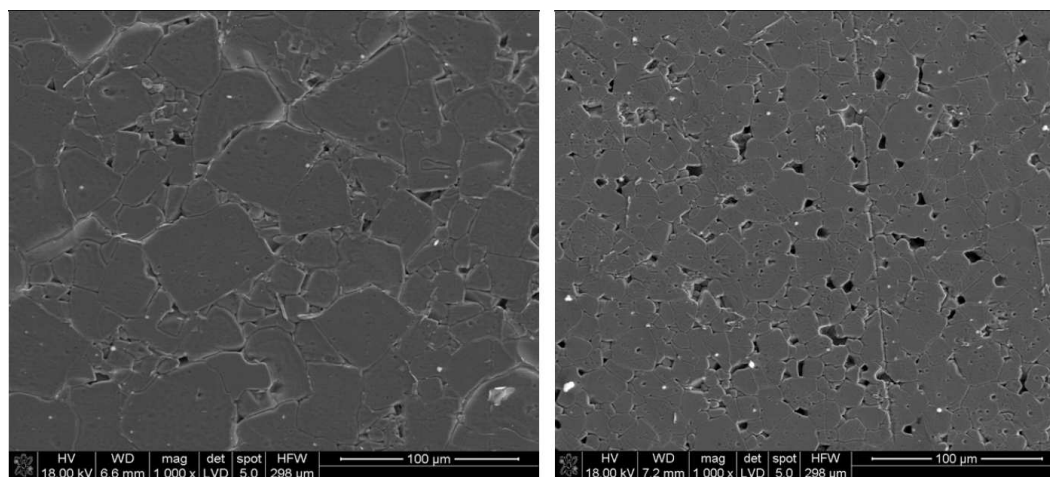

Figure 1. SEM images for the obtained B1C9TO (a) and B9C1TO (b) ceramics
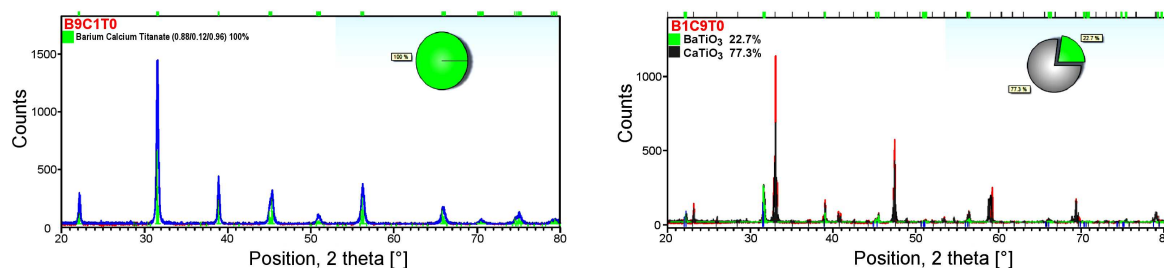
Figure 2. SEM images for the obtained B1C9TO (a) and B9C1TO (b) ceramics

Table 1. XRD related results for the obtained B1C9TO and B9C1TO ceramics

Parameter	B9C1TO	B1C9TO	
	BaTiO$_3$	BaTiO$_3$	CaTiO$_3$
Density measured [g/cm^3]	5.81	4.29	
Density calculated XRD [g/cm^3]	6.1078	4.50	
Lattice parameter, *a* [Å]	3.9778(6)	3.9967(1)	5.4425(2)
Lattice parameter, *b* [Å]	3.9778(6)	3.9967(1)	7.6481(2)
Lattice parameter, *c* [Å]	4.0069(7)	4.0222(2)	5.3970(3)
Unit cell volume, *V* [Å^3]	63.39930	64.24787	224.2327
Space group	*P4mm*	*P4mm*	*Pnma*
GOF	1.9	1.4	1.4

ics shows grains with partially large size, even with the size of over 50 μm, that are surrounded by much smaller grains suggesting biphasic structure with barium titanate and calcium titanate grains (Fig. 1a). On the other hand, the sample B9C1TO has a homogeneous microstructure with an average grain size of 23 μm indicating on the single phase structure. However, this ceramics has a higher amount of inter-crystalline porosity than the sample B1C9TO (Fig. 1b).

After sintering, shrinkage was measured and it was equal to 13 ± 1.2% and 15 ± 1.2% for the Pr-doped Ba$_{0.9}$Ca$_{0.1}$TiO$_3$ and Ba$_{0.1}$Ca$_{0.9}$TiO$_3$ ceramics, respectively, so that the densification process is almost complete.

3.2. XRD characterization

The literature data confirmed [18,19] that a pure tetragonal phase is present in the ceramics with low Ca content (0–0.25), and two-phase tetragonal/orthorhombic structure was observed for the samples with higher calcium content. Figure 2a shows the XRD pattern of the B9C1TO ceramics with practically no difference in the form compared to the calculated formula from the PDF database (for barium calcium titanate 0.88/0.12/0.96)). Consequently, the Goodness of Fit (*GOF*) parameter in this case was almost ideal and equal to *GOF* = 1.9. Thus, the B9C1TO sample shows a tetragonal perovskite phase (*P4mm* space group) without any secondary phase.

In Fig. 2b evolution of strong new peak, i.e. at around 33° (2*θ*) in the sintered B1C9TO sample is clearly seen. Several additional peaks are also visible for this high Ca doping concentration, so that the material becomes biphasic (tetragonal BaTiO$_3$ + orthorhombic CaTiO$_3$).

The lattice parameters for both forms were calculated using the Rietveld method from all peaks of tetragonal structure and results are shown in Table 1. It can be seen that the reduction in unit cell size and volume is probably due to the replacement of Ba^{2+} ion with the smaller Ca^{2+} ion in the Ba$_{0.1}$Ca$_{0.9}$TiO$_3$ structure in comparison to the Ba$_{0.9}$Ca$_{0.1}$TiO$_3$ one.

3.3. Temperature induced dielectric properties

Figure 3 shows dielectric spectra at different frequencies of both BCT samples measured near the Curie temperature. The peak of dielectric permittivity has a narrow shape for the B9C1TO ceramics and reaches the value of 10856 at the Curie temperature (*T$_C$*) of 395 K (Fig. 3a), which is significantly higher than reported in the literature [20,21].

On the other hand, completely flat characteristics for the Curie temperature range were recorded in the B1C9TO sample containing only 10% of ferroelectric BaTiO$_3$ phase (Fig. 3b). The same effect is reflected in the dielectric loss tangent spectra, so that the B9C1TO ceramics reflects clear maxima shortly below *T$_C$*, but the B1C9TO sample does not (Figs. 3c and 3d).

To sum up, the wet chemistry method used gives such a large increase in dielectric permittivity in *T$_C$*, confirming exceptionally pure ferroelectric phase in the case of Ba$_{0.9}$Ca$_{0.1}$TiO$_3$ ceramics.

3.4. Ferroelectric properties

As expected, the hysteresis loop as a ferroelectric fingerprint was registered only for the B9C1TO ceramics (Fig. 4). As mentioned above, this characteristic ferroelectric indicator occurs in the form of a sharp peak in the dielectric constant characteristic at 395 K, therefore
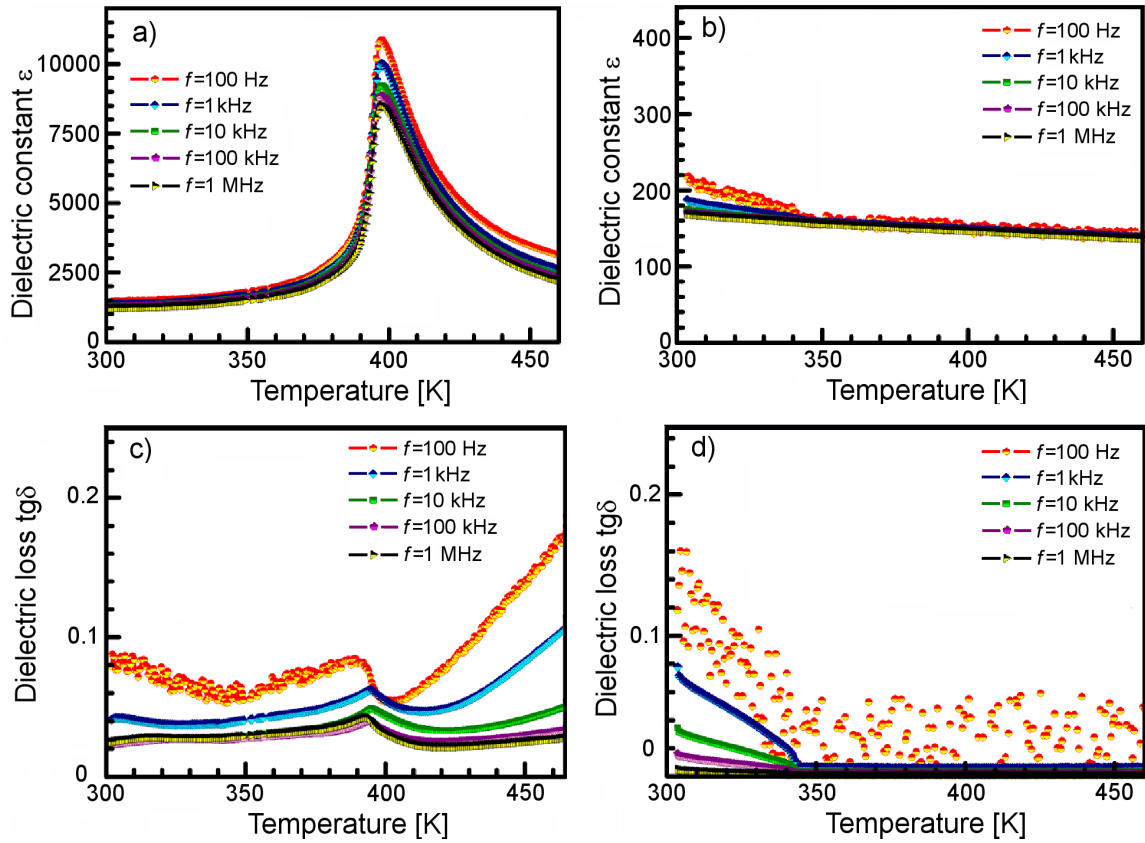
Figure 3. Dielectric characteristics of B9C1TO (a) and (c) and B1C9TO (b) and (d) ceramics
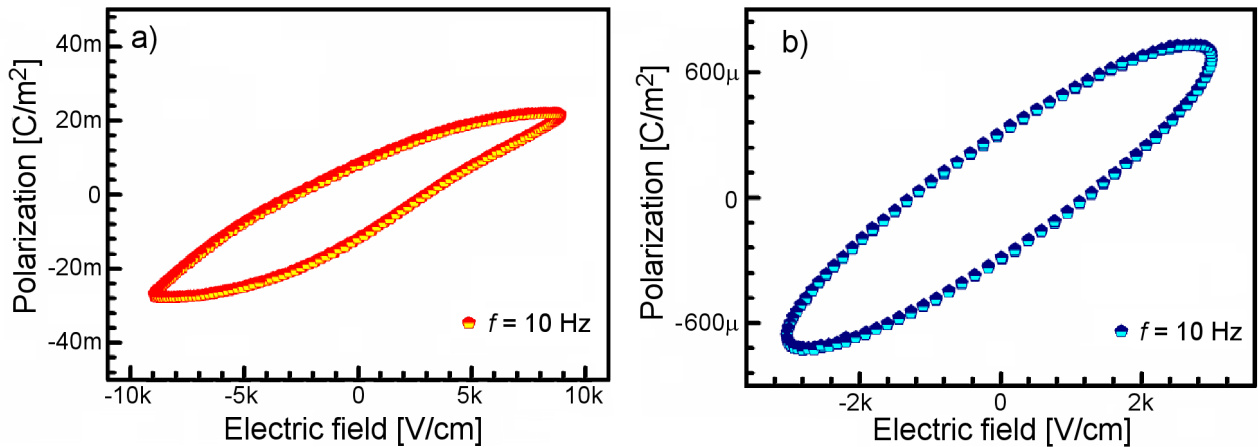

Figure 4. Ferroelectric hysteresis loops for B1C9TO (a) and B1C9TO (b) ceramics

polarization reorientation by electric field is only observed in the BCT ceramics with low calcium content (Fig. 4a).

Generally, however, multivalent cations as praseodymium and oxygen vacancies create sources of residual conductivity, which means that annealing treatment during ceramic processing can significantly rise the conductivity. Thus, this is the reason of asymmetrical shape and not saturated hysteresis loop, as one can see in Fig. 4a.

The remnant polarization defined as the saturation polarization at zero field is $P_R = 10\,\mu C/m^2$, and the coercive field is the field value at zero polarization $E_C = 2.7\,kV/cm$. In the case of the B1C9TO ceramics, only the dielectric response in a form of a circle at *P-E* characteristics is visible without traces of polarization switching (Fig. 4b).

3.5. Luminescence properties

Luminescence spectra were recorded at room temperature. Emission of red light can be observed with the naked eye when excited by UV light (Fig. 5a). The emission spectrum of the Pr^{3+}-doped $Ba_{0.1}Ca_{0.9}TiO_3$ is presented in Fig. 5b. The emission spectrum shows a strong single emission band reaching a maximum at 615 nm. The position and width of the emission band are the
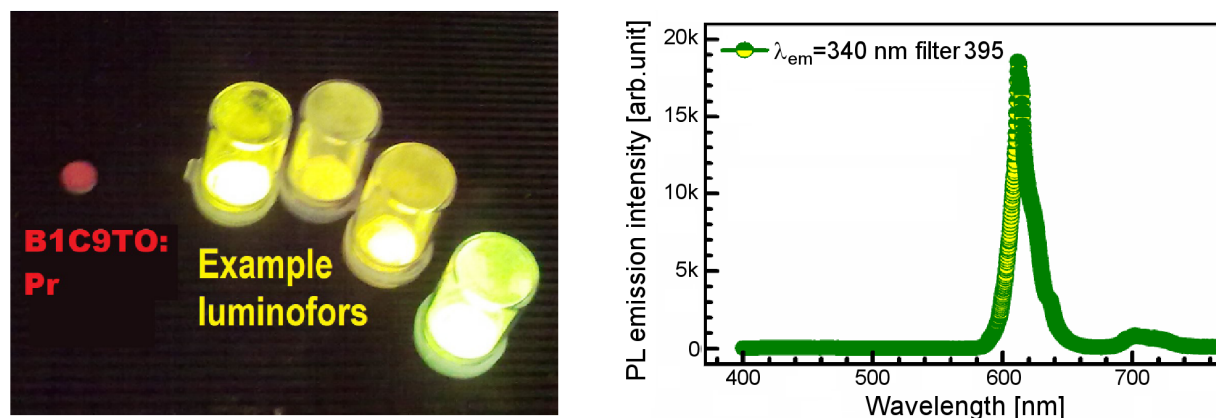
Figure 5. Luminescence (a) and the emission spectrum for $Ba_{0.9}Ca_{0.1}TiO_3$:Pr^{3+} ceramics (b)

same as for the $Ba_{0.77}Ca_{0.23}TiO_3$ doped compound reported by Wang [17]. Thus, the emission band can be assigned to the same luminescent centre – the $^1D_2 - {}^3H_4$ transition of $Pr_3{}^+$ in the $CaTiO_3$ based host.

IV. Conclusions

In this work wet chemistry method was used for the preparation of Pr-doped BCT ($Ba_{0.9}Ca_{0.1}TiO_3$ and $Ba_{0.1}Ca_{0.9}TiO_3$) powders and the corresponding ceramics were prepared after uniaxial compression and sintering at 1500 °C for 2 h. The resulting ceramics showed high relative density, reasonable dielectric and ferroelectric properties. The peak of dielectric permittivity has a narrow shape for the Pr-doped $Ba_{0.9}Ca_{0.1}TiO_3$ and reaches the value $\varepsilon' = 10856$ at the Curie temperature (395 K), which is significantly higher than from mixed oxide method reported in the literature. For the first time, luminescence was recorded in $Ba_{0.9}Ca_{0.1}TiO_3$, despite reports that light emission in BCT is probably only over 23% calcium content, and the red light emission can be observed with the naked eye.

References

1. N. Terasaki, C.N. Xu, "Mechanoluminescence recording device integrated with photosensitive material and europium-doped $SrAl_2O_4$", *Jpn. J. Appl. Phys.*, **48** (2009) 04C150.
2. N. Terasaki, C.N. Xu, "Historical-log recording system for crack opening and growth based on flexible sensor", *IEEE Sens. J.*, **13** (2013) 3999–4004.
3. N. Terasaki, Y. Fujio, Y. Sakata, S. Horiuchi, H. Akiyama, "Visualization of crack propagation for assisting double cantilever beam test through mechanoluminescence", *J. Adhesion.*, **94** (2018) 867–879.
4. N. Terasaki, C.-N. Xu, C. Li, L. Zhang, Y. Sakata, N. Ueno, C.-N. Xu, K. Yasuda, L.H. Ichinose, "Fatigue crack detection of steel truss bridge by using mechanoluminescent sensor", pp. 2542–2549 in *Bridge Maintenance, Safety, Management, Resilience and Sustainability: Proceedings of the Sixth International IABMAS Conference*, Ed. F. Biondini, D.M. Frangopol. Stresa, Lake Maggiore, Italy, 2012.
5. N. Terasaki, C. Xu, C. Li, L. Zhang, C. Li, D. Ono, M.

6. Tsubai, Y. Adachi, Y. Imai, N. Ueno, T. Shinokawa, "Visualization of active crack on bridge in use by mechanoluminescent sensor", *Proceedings 8348 Health Monitoring of Structural and Biological Systems*, (2012) 83482D.
6. C.N. Xu, N. Ueno, N. Terasaki, H. Yamada, *Mechanoluminescence and Novel Structural Health Diagnosis*, NTS Shuppan, Tokyo, 2012.
7. Y. Zuo, X. Xu, X. Tao, X. Shi, X. Zhou, Z. Gao, X. Sun, H. Peng, "A novel information storage and visual expression device based on mechanoluminescence", *J. Mater. Chem. C*, **7** (2019) 4020–4025.
8. A. Feng, F. Philippe, "A review of mechanoluminescence in inorganic solids: Compounds, mechanisms, models and applications", *Smart Mater.*, **11** [4] (2018) 484–489.
9. K.K. Yan, T. Miyamoto, M. Adachi, "Lead-free piezoelectric ceramics with large dielectric and piezoelectric constants manufactured from $BaTiO_3$ nano-powder", *Jpn. J. Appl. Phys.*, **46** (2007) L97.
10. X Wang, H. Yamada, C-N. Xua, "Large electrostriction near the solubility limit in $BaTiO_3$-$CaTiO_3$ ceramics", *Appl. Phys. Lett.*, **86** (2005) 022905–022911.
11. Q. Yang, L. Fang, F. Zheng, M. Shen, "Structural, electrical, luminescent, and magnetic properties of $Ba_{0.77}Ca_{0.23}TiO_3$:Eu ceramics", *Mater. Chem. Phys.*, **118** (2009) 484–489.
12. J.G. Park, T.S. Oh, Y.H. Kim, "Dielectric properties and microstructural behaviour of B-site calcium-doped barium titanate ceramics", *J. Mater. Sci.*, **27** (1992) 5713–5719.
13. M.R. Panigrahi, S. Panigrahi, "Structural analysis of 100% relative intense peak of $Ba_{1-x}Ca_xTiO_3$ ceramics by X-ray powder diffraction method", *Physica B*, **405** (2010) 1787–1791.
14. G. Singh. V. Tiwari, P. Gupta, "Thermal stability of piezoelectric coefficients in $(Ba-Ca)(Zr_{0.05}Ti_{0.95})O_3$, lead-free piezoelectric ceramic", *Appl. Phys. Lett.*, **102** (2013) 162905–162913.
15. L. Zhang, L. Ben, O.P. Thakur, A. Feteira, A.G. Mould, D.C. Sinclair, A.R. West, "Ferroelectric aging and recoverable electrostrain in $BaTi_{0.98}Ca_{0.02}O_{2.98}$ ceramics", *J. Am. Ceram. Soc.*, **91** (2008) 3101–3104.
16. V.S. Puli, A. Kumar, D.B. Chrisey, M. Tomozawa, J.F. Scott, R.S. Katiyar, "Barium zirconate-titanate/barium calcium-titanate ceramics via sol-gel process: Novel high-energy-density capacitors", *J. Phys. D Appl. Phys.*, **44** (2011) 395403–395409.
17. X. Wang, C.-N. Xu, H. Yamada, K. Nishikubo, X.-

G. Zheng, "Electro-mechano-optical conversions in Pr^{3+}-doped BaTiO$_3$-CaTiO$_3$ ceramics", *Adv. Mater.*, **17** (2005) 1254–1258.

18. J.S. Park, Y.H. Lee, K.B. Kim, Y.I. Kim, "Structural study of Ca doped barium titanate", *Nucl. Instr. Meth. B*, **284** (2012) 44–48.

19. X. Cheng, M. Shen, "Different microstructure and dielectric properties of Ba$_{1-x}$Ca$_x$TiO$_3$ ceramics and pulsed-laserablated films", *Mater. Res. Bull.*, **42** (2007) 1662–1668.

20. P.S.R. Krishna, D. Pandey, V.S. Tiwari, R. Chakravarthy, B.A. Dasannacharya, "Effect of powder synthesis procedure on calcium site occupancies in barium calcium titanate: A Rietveld analysis", *Appl. Phys. Lett.*, **62** (1993) 231–239.

21. M.R. Panigrahi, S. Panigrahi, "Diffuse phase transition and dielectric study in Ba$_{0.95}$Ca$_{0.05}$TiO$_3$ ceramic", *Physica B*, **405** (2010) 2556–2559.